Molecular Vision 2020; 26:378-391 <http://www.molvis.org/molvis/v26/378>
Received 20 January 2020 | Accepted 19 May 2020 | Published 21 May 2020

© 2020 Molecular Vision

Analysis of variants in Chinese individuals with primary open-angle glaucoma using molecular inversion probe (MIP)-based panel sequencing

Ting Liu,[1] Chao Tang,[2] Xiaolong Shi[2]

[1]Department of ophthalmology, Daping Hospital of the Army Medical University, Chongqing, China; [2]Radiation & Cancer Biology Laboratory, Oncology Radiotherapy Center, Chongqing University Cancer Hospital & Chongqing Cancer Institute & Chongqing Cancer Hospital, Chongqing, China

Purpose: Family-based genetic linkage analysis and genome-wide association studies (GWASs) have identified many genomic loci associated with primary open-angle glaucoma (POAG). Several causative genes of POAG have been intensively analyzed by sequencing in different populations. However, few investigations have been conducted on the identification of variants of coding region in the genes identified in GWASs. Therefore, further research is needed to investigate whether they harbor pathogenically relevant rare coding variants and account for the observed association.
Methods: To identify the potentially disease-relevant variants (PDVs) in POAG-associated genes in Chinese patients, we applied molecular inversion probe (MIP)-based panel sequencing to analyze 26 candidate genes in 235 patients with POAG and 241 control subjects.
Results: The analysis identified 82 PDVs in 66 individuals across 235 patients with POAG. By comparison, only 18 PDVs in 19 control subjects were found, indicating an enrichment of PDVs in the POAG cohort (28.1% versus 7.9%, p = 8.629e-09). Among 26 candidate genes, the prevalence rate of PDVs in five genes showed a statistically significant difference between patients and controls (33 out of 235 versus 1 out of 241, p = 4.533e-10), including *ATXN2* (p = 0.0033), *TXNRD2* (p = 0.0190), *MYOC* (p = 0.0140), *FOXC1* (p = 0.0140), and *CDKN2B* (p = 0.0287). Furthermore, two sisters harboring a stop-loss mutation *EFEMP1* p.Ter494Glu were found in the POAG cohort, and further analysis of the family strongly suggested that *EFEMP1* p.Ter494Glu was a potentially disease-causing mutation for POAG. A statistically significant difference in age at diagnosis between patients with PDVs and those without PDVs was found, implying that some of the identified PDVs may have a role in promoting the early onset of POAG disease.
Conclusions: The results suggest that some of the associations identified in POAG risk loci can be ascribed to rare coding variants with likely functional effects that modify POAG risk.

Glaucoma is a complex progressive neurodegenerative eye disease caused by genetic and environmental factors [1]. It is the leading cause of irreversible blindness worldwide. There are an estimated 57.5 million people worldwide with glaucoma [2]. It was estimated recently that there will be approximately 79.6 million people with glaucoma by 2020 [3,4]. Based on anatomic changes in the anterior chamber angle, primary glaucoma may be classified as primary angle closure glaucoma (PACG) or primary open-angle glaucoma (POAG). POAG is the most common form of glaucoma which is clinically characterized by an open and normal anterior iridocorneal chamber angle and responsible for 74% of all glaucoma cases, affecting 1% to 2% of the population over age 40 [4]. POAG may be further subdivided into juvenile open-angle glaucoma (JOAG) and adult onset POAG [5]. JOAG is an uncommon subset of POAG that differs from adult-onset POAG in the age of onset and often in the magnitude of intraocular pressure (IOP) elevation.

Family pedigree studies have indicated that some portion of glaucoma is inherited in a Mendelian pattern. Family-based genetic linkage analysis has identified many genomic loci associated with POAG, including GLC1A to GLC1P, and GLC3A [6,7]. Several causative genes, such as *MYOC* (Gene ID 4653, OMIM 601652) [8,9], *OPTN* (Gene ID 10133, OMIM 602432) [10], *WDR36* (Gene ID 134430, OMIM 609669) [11], *CYP1B1* (Gene ID 1545, OMIM 601771) [12,13], *ASB10* (Gene ID 136371, OMIM 615054) [14,15], and *FOXC1* (Gene ID 2296, OMIM 601090) [16] were discovered. To date, only 5–10% of POAG is attributed to single-gene or Mendelian forms of glaucoma [6]. Many of the other cases of POAG are likely due to the combined effects of several genetic and environmental risk factors. This indicates that many cases of POAG have a more complex genetic basis. In recent years, genome-wide association studies (GWASs) have been used to locate the genetic risk factors that contribute

Correspondence to: Xiaolong Shi, Radiation & Cancer Biology Laboratory, Oncology Radiotherapy Center, hongqing University Cancer Hospital & Chongqing Cancer Institute & Chongqing Cancer Hospital, Chongqing 400030, China; email: xshi.bear@foxmail.com

to the development of glaucoma. GWASs have demonstrated many genomic loci are associated with POAG risk, including *CDKN2B-AS1* (Gene ID 100048912, OMIM 613149), *TMCO1* (Gene ID 54499, OMIM 614123), *CAV1* (Gene ID 857, OMIM 601047), *CAV2* (Gene ID 858, OMIM 601048), *SIX1* (Gene ID 6495, OMIM 601205), *SIX6* (Gene ID 4990, OMIM 606326), *AFAP1* (Gene ID 60312, OMIM 608252), *ABCA1* (Gene ID 19, OMIM 600046), *TXNRD2* (Gene ID 10587, OMIM 606448), *FOXC1/GMDS* (Gene ID 2762, OMIM 602884), *ATXN2* (Gene ID 6311, OMIM 601517), *FNDC3B* (Gene ID 64778, OMIM 61190), ABO (Gene ID 28, OMIM 110300), *PMM2* (Gene ID 5373, OMIM 601785), *ATOH7* (Gene ID 220202, OMIM 609875), *TMCO1* (Gene ID 54499, OMIM 614123), and *GAS7* (Gene ID 8522, OMIM 603127) [1,6]. GWASs use single nucleotide polymorphism (SNP) markers to locate the new susceptibility gene; therefore, GWASs rarely identify functional or causal variants and cannot provide direct information on mutation patterns of susceptive genes. Mutation screening of the candidate genes is crucial for implicating the genes as the cause of a particular disease. Currently, several causative genes, such as *MYOC, OPTN, WDR36, CYP1B1, ASB10, FOXC1*, and *PITX2* (Gene ID 5308, OMIM 601542), have been intensively analyzed by sequencing in different populations [8-12]. However, for the genes identified in GWASs, little information for variants detected in coding regions is available. Therefore, further research is needed to investigate whether these genes harbor pathogenically relevant rare coding variants and account for the observed association.

Recent advances in high-throughput sequencing technologies have dramatically improved the efficiency of screening for mutations in genes. Target sequencing for multiple candidate genes has become an important strategy for cost-effective detection of all possible mutations [17,18]. In this study, we used molecular inversion probe (MIP)-based panel sequencing technology to identify rare coding variants associated with POAG. This technology enables high-throughput sequencing for coding regions of multiple candidate genes [18]. Furthermore, all steps of enriching the target area with an MIP can be performed in one test tube, so it is suitable for the screening of a large number of samples. In this study, a 26-gene panel were designed for analysis of the coding variants. This panel contained several POAG-causing genes, such as *MYOC*, *OPTN*, *WDR36*, *ASB10*, and *CYP1B1*, and many genes identified in GWASs or in association studies using the candidate-gene approach, such as *ABCA1, AFAP1, ABO, ATXN2, ATOH7, CAV1, CAV2, CDKN2B* (Gene ID 1030, OMIM 600431), *LOXL1* (Gene ID 4016, OMIM 153456), and *APOE* (Gene ID 348, OMIM 107741). In addition, we included several candidate genes for research on their putative role in POAG, such as *LOXL1,* which has been reported with exfoliation glaucoma [19]; *EFEMP1,* which was identified by exon sequencing of families with POAG [20]; *PAK7* (Gene ID 57144, OMIM 608038), which has shown copy number variation (CNV) in patients with POAG [21]; and *VRK2* (Gene ID 7444, OMIM 602169), which is located in 2p15-p16 which was associated with POAG in a previous study we conducted [22]. By applying this panel, we performed the identification of potentially disease-relevant variants (PDVs) in 235 Han Chinese patients with POAG and 241 controls. We identified numerous variants of interest for further analysis.

METHODS

Sample collection: This study was approved by the ethics committee of Daping Hospital of the army medical university. All experimental procedures were conducted in accordance with the Association for Research in Vision and Ophthalmology (ARVO) statement on human subjects. All participants signed an informed consent form before participating in the study in accordance with the provisions of the Declaration of Helsinki. A total of 235 patients with POAG and 241 unrelated control subjects without glaucoma were recruited at the Third Affiliated Hospital (Daping Hospital) of the Army Medical University from January 2018 to December 2018. All patients were assigned a study identity number that was known only to the ophthalmologist in the researcher group. These numbers were subsequently converted to linked study identities such that others could not access patients' private information. All human samples were linked to the study identities and barcoded, anonymized, and tracked in a centralized database, which was overseen by the researchers.

Most of the 235 patients are sporadic cases except the one set of siblings reported in this study (Appendix 1). All patients were Han Chinese. Patients with POAG were diagnosed by glaucoma specialists and fulfilled the following diagnostic criteria: open angles on gonioscopy (Grade 3 or 4 in Shaffer classification); presence of glaucomatous optic disc changes, including high cup-disc ratios (CDRs were estimated by one experienced doctor (T.L.) under ophthalmoscopy), disc ratio asymmetry between eyes (>0.2), vertical elongation of the cup, focal neuroretinal rim thinning or notching, beta-zone peripapillary atrophy; abnormal circum papillary retinal nerve fiber layer (RNFL) thickness (cpRNFLT) in at least one clockwise optical coherence tomography (OCT) scan sector between 6, 7, 8, 10, 11, and 12 o'clock (6, 5, 4, 2, 1, and 12 o'clock in the left eye), confirmed in at least three examinations; visual field abnormalities, including localized defects respecting the horizontal meridian, nasal step, arcuate scotoma; and abnormal standard automated perimetry (SAP)

tests were defined as pattern standard deviation (PSD) outside 95% normal confidence limits, or glaucoma hemifield test (GHT) outside normal limits (Humphrey, Zeiss, Germany), confirmed in at least two examinations. Exclusion criteria were the following: finding of secondary glaucoma (exfoliation syndrome, etc.) and any other ocular or systemic disease that could affect the optic nerve or the visual field.

The 241 unrelated control subjects ranged in age from 38 to 78 years, average age 63.7, and were confirmed without glaucoma symptoms. The clinical details of the 235 patients and the 241 control subjects are summarized in Table 1 (for more information, also see Appendix 1 and Appendix 2).

MIP design: Twenty-six candidate genes were chosen for mutation screening in the patients with POAG. The candidate genes are listed in Appendix 3, and previous studies are summarized in Appendix 3. A total of 684 MIP oligonucleotides were designed to cover 314 exons (Appendix 4). The target DNA size was about 54 K bases. The MIPs were manually designed to capture the coding regions and 20- to 50-bp flanking regions of the exons of the target genes. The general structure for the MIP is a common 41-bp linker flanked by an extension and a ligation arm of 16 to 28 bp. The extension and ligation arms were designed with Tm of 57–62 °C. The MIP targets a specific 120–140 bp genomic region for gap-fill and circularization.

Target capture: Individual MIPs were column synthesized (SBS Genetech, Beijing, China). MIP capture experiments were performed with some modifications as previously described [18]. In briefly, a total of 684 probes were pooled and phosphorylations were performed with ATP and Polynucleotide Kinase (NEB, Beijing, China). Pooled probes used as a master probe mix. The genomic DNA was sheared into 300-500 bp by Bandelin sonorex AK 102 sonicator (Bandelin, Berlin, Germany) and then MIPs were added to hybridization mixture (300 ng fragmented DNA, 1× Ampligase buffer). Hybridization procedure was conducted as fellows: 94 °C for 2 min, 54 °C for 36 h. And then gap filling-in reaction was conducted as fellows: 0.3 µl Phusion DNA polymerse (NEB), 0.6 µl Ampligase (Epicentre, Madison) and 0.1 µM dNTP (NEB) was added for filling-in the gap at 54 °C for 3 h. To degrade un-circularized DNA, 0.5 µl Exonuclease I (NEB) and 0.5 µl Exonuclease III (NEB) was added to reaction mixture at 37 °C for 45 min, and then exonucleases were inactivated at 94 °C for 4 min.

Amplification and sequencing of the target library: Five microliters of circularized DNA was used for amplification in a 25-µl reaction containing 0.1 µM of the truncated PE1.0 primer and the PU primer with the Illumina adaptor sequence, 0.6 U of Phusion DNA polymerase, 200 µM of each dNTP, and 1X Phusion Master Mix. The first round of PCR was performed at 98 °C for 30 s, 13 cycles of 98 °C for 10 s, 57 °C for 30 s, 72 °C for 15 s, and finally 72 °C for 5 min. Then 5-µl reaction mixture containing 0.5 µM Illumina PE1.0 primer and sample index primer was added to the first-round PCR mixture to perform an additional PCR at 98 °C for 30 s, 13 cycles of 98 °C for 10 s, 59 °C for 30 s, 72 °C for 15 s, and finally, 72 °C for 5 min (primer sequences are listed in Appendix 4). Barcoded libraries were pooled together and purified with 0.8X AMPure XP beads (Beckman Coulter, Brea, CA) to remove the primer dimers. The purified library was sent for sequencing of 2X 150-bp paired-end reads on Illumina Hiseq X-Ten (San Diego, CA).

Sequencing data analysis and variant identification: Before alignment, low-quality reads were removed with filtering. All reads were aligned to the human reference genome (GRCh37/hg19) using the Burrow Wheeler Aligner (BWA)-Smith Waterman (SW) algorithm from BWA software version 0.7.15, with all alignment parameters set to default values. Resulting alignments were processed and converted to the BAM format with SAMtools software version 0.1.18.22. The sequence variants were called by the GATK and Picard programs (https://software.broadinstitute.org/gatk/) and further annotated by wAnnovar and Ensembl Variant Effect Predictor (VEP). Sequence alignments at variant positions were manually inspected using Integrative Genomics Viewer (IGV) software version 2.3.90. An average of about 0.2 Gb per sample (range 0.1–0.4 Gb per sample) of high-quality sequences was obtained. In this study, several optimizations were employed to improve the efficiency and uniformity of capture of the MIPs (Appendix 5). The approach achieved a high on-target specificity that about 91% of total reads can be mapped to the target regions. Targeted sequencing yielded median about 1,000-fold coverage; 98.4% of bases had >50-fold coverage. Twelve variants were selected for confirmation, and all showed agreement with the results with Sanger sequencing (Appendix 5).

We selected rare variants for further analysis that met the following criteria: i) The variant was present in sequence reads from both strands, and the sequencing depth at the variant was more than 30; ii) the variant had a minor allele frequency (MAF) <0.01 in the 1000 Genomes Project database (variants with minor allele frequency <0.03 in the East Asian populations of Exome Aggregation Consortium (ExAC_EAS) were filtered out); iii) the variant represents at least 20% of the sequence reads at a particular site; and vi) all synonymous variants were not included.

In order to identify the PDVs from the identified rare variants (Appendix 6 and Appendix 7), we adopted the

Table 1. Demographic and clinical features of the study subjects.

Demographic/clinical features	POAG	With-PDVs	without-PDVs	P value	Controls	With-PDVs	Without-PDVs	p- value
N (M/F)	235(114/121)	66 (28/38)	169 (86/83)	-	241 (111/130)	19(11/8)	222(100/122)	-
Age* (years)	52.7±14.5	44.8±14.6	55.8±13.2	5.37E-07	63.7±6.9	65.3±6.0	63.5±7.0	0.2527
Age range	17–79	17–75	17–79	-	43–78	47–75	43–78	-
≤40 years (N)	50	27	23	1.26E-05	0	0	0	1
40–60 years (N)	91	26	65	1	76	3	73	0.1965
≥60 years (N)	94	13	81	5.81E-05	165	16	149	0.1965
IOP (mmHg)	25.6±10.1	26.5±9.9	25.3±10.2	0.4062	14.8±2.1	14.8±2.8	13.7±1.9	0.0812
cup-disc ratio	0.70±0.21	0.72±0.22	0.69±0.20	0.3366	0.28±0.04	0.27±0.05	0.29±0.04	0.2989
Mean RNFLT	64.1±11.9	63.5±10.6	64.3±12.4	0.5904	105.2±8.0	106.4±7.3	105.1±8.1	0.4931
Mean Defect	−16.4±9.1	−14.9±9.9	−16.9±8.6	0.1349	−2.4±0.9	−2.3±0.9	−2.4±0.9	0.761

*Age at diagnosis for POAG patients or age at participating the project for control subject.

analysis procedure used in the previous literature to filter variants [23,24]. The variants that occurred in the control group and did not reach a statistically significant difference (p>0.05) between the patient and control groups were excluded. Variants, such as nonsense, frame-shift, canonical ± one or two splice sites, stop codon loss, deletion, and initiation codon loss, were included [25]. Two in silico tools, PolyPhen2 [26] and Sorting Intolerant From Tolerant (SIFT) [27], which have been recommended for aiding in the interpretation of sequence variants [25], were used to predict potentially deleterious effects of the variants. We filtered out the missense variants that were considered to be "tolerated" or "deleterious with low confidence" by SIFT, and were considered to be "benign" or "possibly damaging" by PolyPhen2 HVAR. Missense variants predicted to be deleterious by either SIFT or PolyPhen2 HVAR were included. Two in-frame deletion mutations predicted to be neutral by SIFT-Indel were also excluded. Five variants also occurred in the Han Chinese population in the 1000 Genomes Project (including 103 individuals of Han Chinese in Beijing (HCB) and 105 South Han Chinese (SHC), Appendix 8) and did not reach statistically significant difference were also excluded. Visualization of protein lollipop structures was performed by using MutationMapper.

Statistical analysis: The frequencies of PDV carriers between patients with POAG and controls in each gene were compared with Fisher's exact test. The clinical features of the study subjects including age at diagnosis (years), IOP, cup-disc ratio, mean RNFLT, and mean defect between the group with PDV and without PDV in the patients and controls were statistically analyzed using the Welch two-sample *t* test, all p values were based on two-tailed statistically analyses, and p values less than 0.05 were considered statistically significant. All analyses were performed with R version 3.5.1.

RESULTS

In this study, 235 patients with POAG and 241 controls were included for variant analysis. The demographic and clinical characteristics of the participants are shown in Table 1. Overall, the mean age of the control group was older than that of the patient group, considering the possible association between the onset of POAG and the age of the individuals. Control individuals were carefully checked to exclude those with any symptoms of POAG. We selected 26 candidate genes for identification of PDVs in POAG based on previous studies (Appendix 3). These candidate genes were chosen for target sequencing analysis as they were reported to be involved in the etiology of eye diseases or were reported to be associated with POAG by GWASs. We analyzed the coding regions for these candidate genes by using MIP-based target sequencing. The workflow of the MIP-based assay is shown in Figure 1.

Two filters were mainly used for identifying the PDVs: allele frequency and in silico tools' predictions of variants. We found 180 rare variants in 143 individuals among 235 patients with POAG and 57 rare variants in 94 individuals among 241 control subjects in coding regions of 26 genes (MAF<0.01, Appendix 6 and Appendix 7). All rare variants identified are heterozygous. Twenty-two rare variants were present in patients with POAG and the controls. However, no statistically significant differences for these 22 rare variants in the allele frequencies were found between the patient and control groups (p>0.11, Fisher's exact test). After further filtering (see Methods), we identified 82 PDVs and 18 PDVs in the patients with POAG and the controls, respectively (Table 2, detailed information was shown in Appendix 9 and Appendix 10). Of the 235 patients with POAG evaluated, 66 (28.1%) had at least one PDV in the candidate genes. In comparison, 19 of 241 subjects harbored PDVs in the control group, indicating an enrichment of PDVs in the POAG cohort (28.1% versus 7.9%, p = 8.629e-09, Fisher's exact test; Appendix 9).

Of the 82 PDVs, there were five known deleterious missense mutations that were reported in previous studies, including p.Gln337Arg [28], p.Gln368Ter [29], and p.Pro370Leu in *MYOC* [30], p.Leu107Val in *CYP1B1* [31], and p.Arg130Trp in *PITX2* [32]. Thus, most of the PDVs identified in this study are novel. Insertions and deletions in the gene-coding regions, stop gain or loss, and variants located at the essential splice site sequences were generally considered to be more likely pathogenic [25]. We found eight such mutations in the POAG cohort, including three truncating mutations (p.Arg272Ter and p.Gln368Ter in *MYOC*, and p.Tyr848Ter in *FNDC3B*), four frame-shift mutations (p.(Asp677fs) in *ABCA1*, p.(Ser267fs) in *APOE*, p.(Gly77fs) in *CDKN2B* and p.(Gly453fs) in *FOXC1*), and a stop-loss mutation p.Ter494Glu in *EFEMP1* in the POAG cohort. Only one control subject harbored such a deleterious mutation (*ABCA1* p.Asp1894Efs) (3.4% versus 0.4%, p = 0.019, Fisher's exact test). Of the 82 PDVs, 74 PDVs were missense PDVs. All PDVs identified in the POAG cohort have low frequencies in the population (<0.3% in ExAC_EAS and 1000 Genome Project database). Four of 82 PDVs were found in two or more patients (*ATXN2* p.Arg939Gln, three cases; *TXNRD2* p.Gly290Val, three cases; *EFEMP1* p.Leu451Pro, two cases; *PAK7* p.Gly310Glu, two cases). However, there was no statistically significant difference in the frequency for each recurrent PDV between the patient group and the control group (p>0.12, Fisher's exact test).

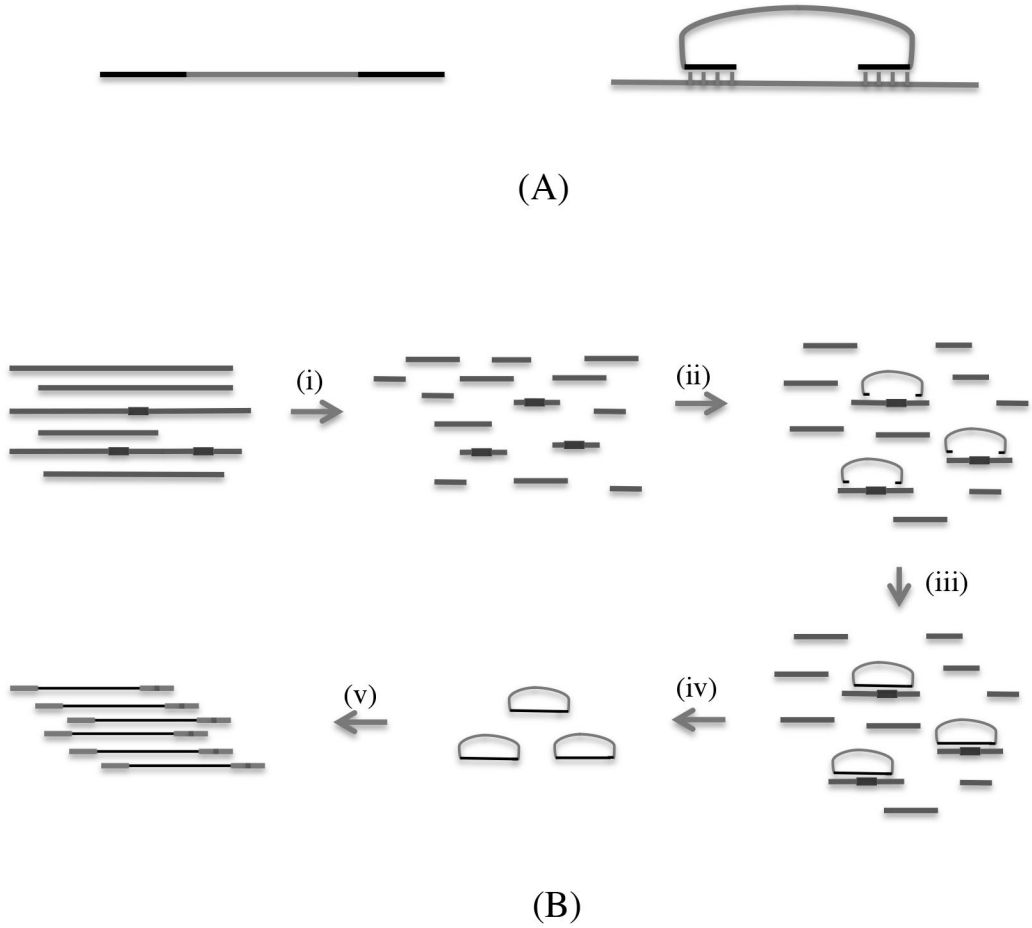

Figure 1. Design of molecular inversion probe and MIP-based target-sequencing workflow. **A**: Molecular inversion probe (MIP) structure and design for regions of interest. The general structure for the MIP is a common 41-bp linker flanked by a target-specific extension and a ligation arm of 16 to 28 bp. **B**: MIP-based target-sequencing workflow. (i) Genomic DNA was sheared into 300–500 bp fragments. (ii) Pooled probes are added to the genomic DNA, and each probe is hybridized to the target DNA sequences through the target-specific sequences on both ends. (iii) The gaps are filled and circularized with DNA polymerase and ligase. (iv) The linear genomic DNA and uncircularized padlock probes are removed with exonuclease. (v) The circularized probes are amplified with a universal sequencing primer and a sample barcode primer.

PDVs were identified in 21 genes among 26 candidate genes for the POAG cohort, including *ATXN2* (six PDVs [7.3% of total PDVs]), *ABCA1* (six [7.3%]), *FOXC1* (six [7.3%]), *LOXL1* (six [7.3%]), *MYOC* (six [7.3%]), *TXNRD2* (six [7.3%]), *CDKN2B* (five [6.1%]), *GAS7* (five [6.1%]), *APOE* (four [4.9%]), *EFEMP1* (four [4.9%]), *FNDC3B* (four [4.9%]), and *PITX2* (four [4.9%]; Appendix 10). Of the 26 genes analyzed, five genes (*ATOH7, SIX6, VRK2, CAV1*, and *CAV2*) had no PDVs in the POAG cohort. Among the 26 candidate genes, the prevalence rate of PDVs in five genes showed a statistically significant difference between the patients and controls, including *ATXN2* (n = 8, 3.4%, p = 0.0033), *TXNRD2* (n = 8, 3.4%, p = 0.0190), *MYOC* (n = 6, 2.6%, p = 0.0140), *FOXC1* (n = 6, 2.6%, p = 0.0140), and *CDKN2B* (n = 5, 2.1%, p = 0.0287). Thirty-three patients harbored PDVs in these five genes, accounting for 50% of the total patients harboring PDVs. In comparison, only one subject with one PDV in these five genes was found in the control group (33/235 versus 1/241, p = 4.533e-10, Fisher's exact test).

Some patients (17 of 66 patients) harbored more than one PDV. For example, five patients with *FOXC1* PDVs also had an additional PDV in *ABCA1, ABO, GAS7*, and *EFEMP1* or two additional PDVs in *AFAP1* and *LOXL1* (Appendix 1). One patient had two different PDVs in *ATXN2* (p.R939Q and p.S1186I). But whether the two PDVs derived from different alleles is unclear. We analyzed the difference in diagnosis

age, IOP, cup-to-disc ratio, mean defect, and mean RNFLT between patients with one PDV and patients with additional PDVs. However, no difference was found in these clinical features.

MYOC is a well-established POAG-causing gene, with a high prevalence rate in patients with POAG, as reported in a previous study [23]. In this study, we found six patients harboring six *MYOC* PDVs, accounting for up to 2.6% of all cases, which is slightly lower than previously reported (2.6% versus 4.6%) [9]. Before filtering against the variants observed in the controls, there were 31 patients harboring rare variants in *MYOC* (an MAF<0.01 in the 1000 Genome Project database), representing the highest rate in the POAG cohort. However, several rare variants also occurred in control subjects. For example, p.Gln19His in *MYOC* has been reported in a previous study [9], which was found in three patients in this POAG cohort and two controls. Furthermore, p.Gln19His was found in three individuals among 208 Chinese individuals in the 1000 Genome Project population (see Appendix 8). These data indicated that p.Gln19His could be considered a polymorphism in the Chinese population. Homozygous p.Arg46Ter in *MYOC* was reported to be pathogenic [33]. Yoon et al. found a homozygous mutation p.Arg46Ter in a Korean patient with JOAG at age 15 years old [33]. In that report, the homozygote with this mutation was severely affected while the father, mother, and a sister were heterozygous for the mutation, apparently without detectable symptoms. This indicated that biallelic inactivation would result in a disease phenotype. In the present study, p.Arg46Ter of *MYOC* occurred in seven patients with POAG and in two control subjects (p = 0.10, Fisher's exact test). These results supported that the heterozygous p.Arg46Ter is a benign variant. Thus, only six PDVs in *MYOC* were identified after filtering. Among these six PDVs, a truncating mutation (p.Arg272Ter), has not been reported in a previous report. We did not find p.Arg272Ter in the EXAC_EAS or 1000 Genomes Project population. We speculated that p.Arg272Ter may be a disease-causing mutation.

In the *WDR36* gene, three PDVs (p.Arg95Gly, p.Ala147Thr, p.Pro780Leu; 1.3%) were found in patients.

Table 2. The potentially disease-causing variants (PDVs) in POAG as compared with control.

Gene	No. with PDVs in POAG (n=235)	No. with PDVs in control (n=241)	p-value	Odds Ratio Cases:Cont (95% CI)
ABCA1	6 (2.6)	7 (3.0)	1	0.88 (0.24-3.10)
ABO	2 (0.9)	0 (0)	0.4989	-
AFAP1	3 (1.3)	0 (0)	0.1203	-
APOE	4 (1.7)	1 (0.4)	0.211	4.14 (0.41-205.29)
ASB10	3 (1.3)	2 (0.9)	1.5439	0.58 (0.18-18.63)
ATXN2	8 (3.4)	0 (0)	0.0033	-
CDKN2B	5 (2.1)	0 (0)	0.0287	-
CYP1B1	1 (0.4)	1 (0.4)	1	1.03 (0.01-80.79)
EFEMP1	5 (2.1)	1 (0.4)	0.1184	5.20 (0.58-247.49)
FNDC3B	4 (1.7)	0 (0.4)	0.0586	-
FOXC1	6 (2.6)	0 (0.4)	0.014	-
GAS7	5 (2.1)	1 (0.4)	0.1184	5.20 (0.58-247.49)
LOXL1	6 (2.6)	1 (0.4)	0.0648	-
MYOC	6 (2.6)	0 (0)	0.014	-
OPTN	2 (0.9)	2 (0.9)	0.6195	1.03 (0.11-121.95)
PAK7	3 (1.3)	2 (0.9)	0.6235	0.68 (0.18-18.63)
PAX6	2 (0.9)	1 (0.4)	0.6195	2.06 (0.11-121.95)
PITX2	4 (1.7)	0 (0.4)	0.0586	-
TMCO1	1 (0.4)	0 (0)	0.4937	-
TXNRD2	8(3.4)	1 (0.4)	0.019	7.34 (0.1-376.19)
WDR36	3 (1.3)	1 (0.4)	0.3672	3.10 (0.25-163.45)

The odds ratio is calculated from the ratio of cases with and without PDVs in each gene in cases divided by the corresponding ratio in controls. P-values were calculated using a two-sided Fisher's Exact Test.

We found that two *WDR36* rare variants, p.Leu240Val and p.Ile713Val, occurred in patients and control subjects (two subjects for p.Leu240Val and three subjects for p.Ile713Val in the patient group; four subjects for p.Leu240Val and six subjects for p.Ile713Val in the control group). Thus, these two variants may be benign. Only two patients with POAG harbored *OPTN* PDVs (p.E230G and p.Val498Asp). This low prevalence rate is comparable with that in other studies on *OPTN* [23].

Investigating whether PDVs occur in the active sites of proteins may be useful to evaluate the influence of alternations on protein function. Locations of PDVs and domains in proteins are shown by lollipop structures (Figure 2). We found several PDVs occurred in the active site of the encoded protein. For *MYOC*, previous studies have demonstrated that most mutations are located in the third exon, which codes for the olfactomedin (OLF)-like domain. The OLF domain contains a high-affinity calcium binding site with a five-bladed β-propeller structure [34]. In this study, we found that all six PDVs identified in the POAG group occurred in the OLF domain, and most were located within or near the calcium binding site. *FOXC1* is a DNA-binding transcriptional factor that is involved in eye development [35]. We found a patient harboring p.Tyr115His in *FOXC1*, which is located in DNA binding sites of *FOXC1* (Figure 2). We deduced that p.Tyr115His may have a strong effect on DNA binding of the transcription factor, which would influence the expression of downstream target genes of *FOXC1*. We found a PDV (p.Cys448Phe) occurred in the *LOXL1* protein lysyl oxidase domain. Cys448 may be a conserved residue because the 443–456 sites are conserved in this domain, and several copper ion binding sites (His449, His451, and H453) are located in this region. Furthermore, Cys448 and Cys497 will form a disulfide bond. The mutation p.Cys448Phe may break the S–S bond. Thus, these variants have a higher probability of damaging the functional impact. The discovery of these PDVs in active sites also provided interesting targets for engineering relevant animal models of glaucoma.

To investigate whether the PDVs influence the symptom of POAG, we analyzed the association between PDVs and clinical features of patients with POAG. There were 66 individuals with PDVs and 169 individuals without PDVs in the patient group (Table 1). The differences in the clinical features between subjects with PDVs and without PDVs were

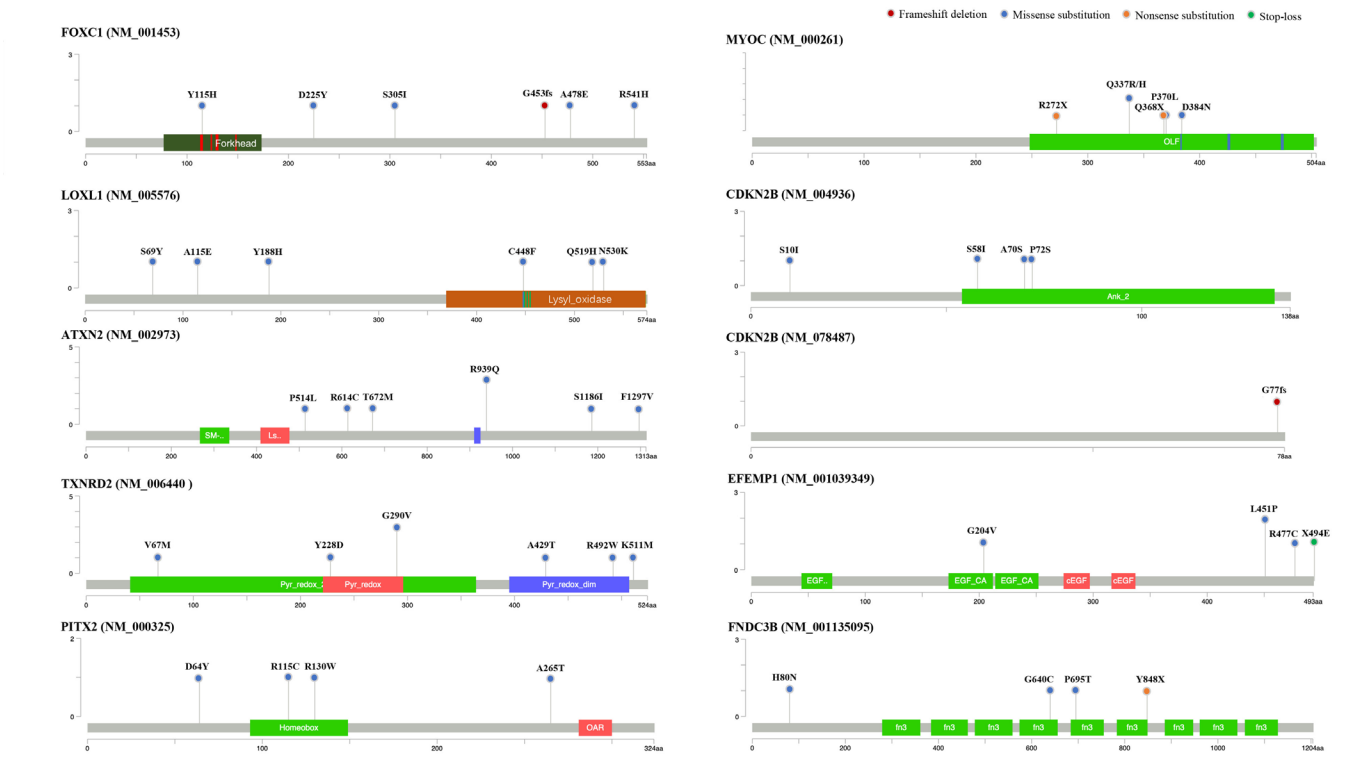

Figure 2. Locations of PDVs and domains in proteins of nine genes are shown by lollipop structures. Sites F114, Y115, N124, R127, H128, and K148 as DNA binding sites are shown with a red line in the forkhead domain of *FOXC1* (UniProt/Q12948). Copper ion binding sites (His449, His451, and H453) located in the lysyl oxidase domain of *LOXL1* are shown with a green line (Uniprot/Q08397). Sites D380, N428, A429, I477, and D478 as calcium ion binding sites are shown with a blue line in the olfactomedin (OLF) domain of *MYOC* (Uniprot/Q99972).

evaluated with a *t* test. No statistically significant difference in the IOP, cup-to-disc ratio, and mean RNFLT were observed between the two groups. We found an association between the presence of PDVs and age at diagnosis (mean of patients with PDVs = 44.8 years, mean of patients without PDVs = 55.8 years, p = 5.37e-07, Welch two-sample *t* test). When classifying patients by age, we found that PDVs were enriched in the subgroup of patients younger than 40 years of age (p = 1.26e-05, Fisher's exact test). It suggests probably a fraction of the PDVs contribute to the development of POAG disease and result in an earlier age of onset for glaucoma. A slight difference in the mean defect was also found (p = 0.1349, Welch two-sample *t* test), indicating that the symptom of the group without PDVs is slightly more severe than that of the group with PDVs. This might be explained by the fact that the subgroup without PDVs is older.

DISCUSSION

Glaucoma is a progressive degenerative condition, and the underlying mechanisms of glaucoma are not well understood. It has been suggested that glaucoma is a complex, multifactorial disease affected by genetic factors and environment [6,36]. Discovery of the potentially disease-relevant variants will facilitate the research of POAG etiology. To discover PDVs in coding regions in a POAG cohort, we developed an MIP-based target sequencing for multiplex genes. This parallel screening for multiple target genes could provide a comparison in their prevalence rate. We found several genes with high prevalence rates that have not been reported in previous studies. Among 26 genes, *TXNRD2* (n = 8, 3.4%) and *ATXN2* (n = 8, 3.4%) had the highest frequency in the POAG cohort, followed by *MYOC* (n = 6, 2.6%), *FOXC1* (n = 6, 2.6%), *LOXL1* (n = 6, 2.6%), *ABCA1* (n = 6, 2.6%), *EFEMP1* (n = 5, 2.1%), *CDKN2B* (n = 5, 2.6%), and *GAS7* (n = 5, 2.1%; Table 2). In particular, we found that five genes, including *TXNRD2*, *ATXN2*, *FOXC1*, *MYOC*, and *CDKN2B*, reached a statistically significant difference between the patient group and the control group. We found that a substantial fraction of PDVs occurred in those genes identified in GWASs, such as *TXNRD2*, *ATXN2*, *FOXC1*, and *CDKN2B*. The *TXNRD2* gene encodes a mitochondrial protein that is involved in the control of reactive oxygen species levels and the regulation of mitochondrial redox homeostasis [37]. Oxidative stress is known to cause retinal ganglion cell (RGC) dysfunction in glaucoma models and clinical glaucoma samples. TXNRD2 regulates the cellular redox environment by scavenging reactive oxygen species in mitochondria [37]. The gene *Ataxin 2* (*ATXN2*) encodes a membrane protein located in the endoplasmic reticulum (ER) and plasma membrane (PM). This protein is involved in endocytosis and modulates mTOR signals that modify ribosomal translation and mitochondrial function [38]. *FOXC1* is a DNA-binding transcriptional factor that plays a role in a broad range of cellular and developmental processes, such as eye, bones, cardiovascular, kidney, and skin development [35]. Mutations in *FOXC1* have been associated with Axenfeld-Rieger (AR) syndrome, a disorder characterized by anterior segment malformations in the eye and glaucoma [39]. A GWAS was performed to identify new susceptibility loci of POAG, and three top SNPs were identified: rs35934224 [T] within TXNRD2; rs7137828 [T] within *ATXN*2, and rs2745572 [A] upstream of *FOXC1* [40]. This study identified new risk loci for POAG. However, whether these candidate genes harbor pathogenically relevant rare coding variants and account for the observed association require further investigation. The present data indicated a high prevalence of potentially pathogenic variants in *TXNRD2* (3.4%), *ATXN2* (3.4%), and *FOXC1* (2.6%) in patients with POAG, providing direct evidence to support the three genes involved in POAG. Furthermore, we found a PDV p.Tyr115His is located in DNA binding sites of *FOXC1* protein that would has a strong influence on protein function. Altogether, these results indicated that a fraction of PDVs may have functional impact on POAG risk loci.

This study indicated that *EFEMP1* might be involved in POAG. Four PDVs of *EFEMP1* were observed in six patients with POAG. Specifically, a stop-loss mutation p.Ter494Glu was found in two sisters with POAG (Figure 3). This stop-loss mutation results in the production of an abnormal protein that is 29 amino acids longer than expected, which may have an impact on its protein function. The siblings also harbored a rare variant p.Arg387Gln in *EFEMP1.* The siblings received a diagnosis of POAG at the age of 21 and 23 years old, respectively. Both exhibited severe visual-field loss in the right eye. Their father also had POAG and was diagnosed at 43 years old. Their mother has not shown any detectable symptoms. Further analysis showed that their father harbored p.Ter494Glu, and their mother harbored p.Arg387Gln (Figure 3). As their father has shown POAG symptoms, we deduced that p.Ter494Glu is the potentially causative mutation for this family. Their mother has p.Arg387Gln, and she does not show any POAG symptoms yet. The missense *EFEMP1* p.Arg387Gln occurred in six patients and eight control subjects, suggesting it might be a normal SNP. The *EFEMP1* gene was located within the GLC1H locus on chromosome 2p (2p15-p16). Although there have been a few efforts to confirm the link to GLC1H, it remains uncertain [41]. It is expressed in the retina and RPE, involved in age-related macular degeneration (AMD) [42,43]. A GWAS identified copy number variation (CNV) at *NPHP1* and *EFEMP1* as

potential candidates for association of inherited retinal degenerative diseases [44]. A report located a genetic locus (GLC1H) for adult-onset POAG maps to the 2p15-p16 region with linkage analysis in an Afro-Caribbean (Jamaican) population [41]. In a previous study, we located a region on chr2 (chr2: 46.4M-65.6M) that contributed to POAG with family-linkage analysis studies in Chinese [22,45], which is overlapped with the 2p15-p16 region. A recent study identified a novel missense variant (p.Arg140Trp) in exon 5 of the gene coding for *EFEMP1* that cosegregated with POAG in an African-American family with exome sequencing [20]. In the present POAG cohort, four *EFEMP1* PDVs occurred in six patients with POAG across 235 patients with POAG, while only one subject with one PDV was found in the control group (2.6% versus 0.4%, p = 0.1184, Fisher's exact test). No other potentially disease-relevant variant in the candidate genes was found in the siblings. The results of the family analysis suggested that *EFEMP1* p.Ter494Glu is a potentially disease-causing mutation, although we cannot completely rule out the possibility that other unexamined sources of mutations contribute to POAG symptoms.

This study not only highlighted the discovery of the novel putative disease-relevant variants for POAG but also provided an effective approach for POAG research. In this study, an MIP-based panel sequencing was used to discover POAG disease-relevant variants. The panel enables automatic and low-cost detection for large POAG samples. In addition, new MIPs can be added to the panel to increase the screening regions. We developed a highly efficient protocol for a large number of samples. The cost of reagent and sequencing is about USD20 per sample for the POAG gene screening with this panel (see Appendix 11). Because MIPs can be used 10,000 times once the probes have been synthesized, the cost per sample would greatly decrease as the sample increases. This cost-saving approach has great potential for evaluating the role of each candidate gene by screening large samples and is suitable for use in a routine mutation screening workflow.

A limitation of the present study is the pathogenicity of the PDVs identified in this study mainly based on the prediction of in silico tools. Further verification with function studies, such as animal models, is required. In this study, in silico tools were used to aid in the interpretation

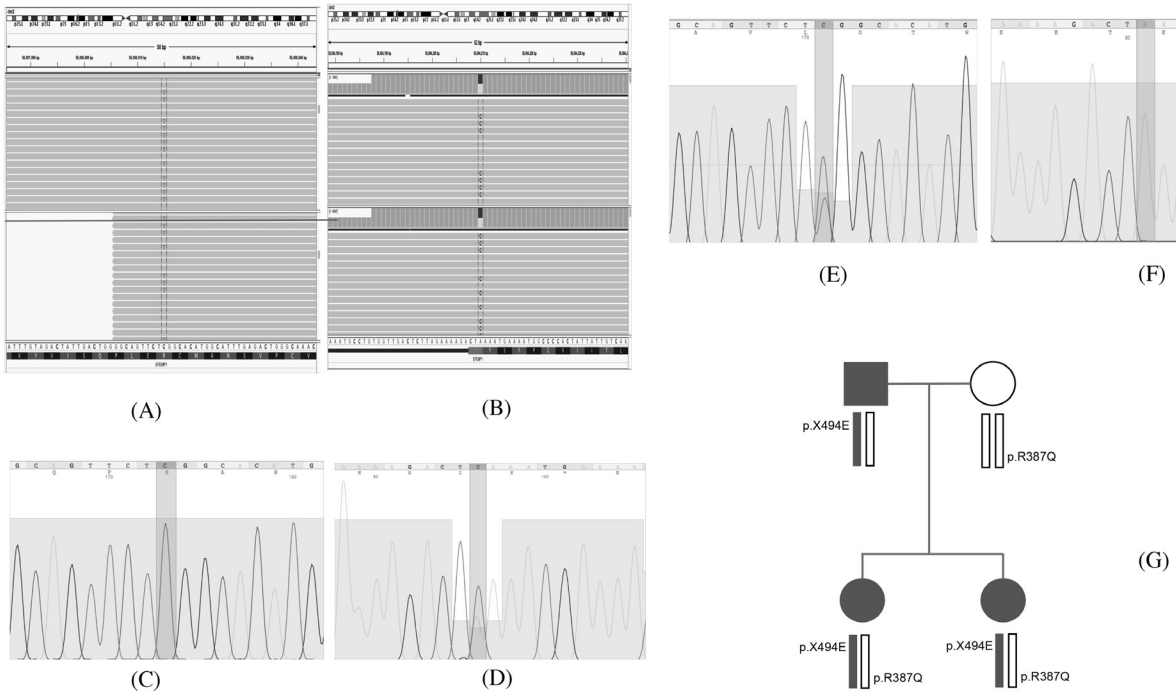

Figure 3. Genetic analysis of a family harboring mutation in *EFEMP1*. Siblings with p.Arg387Gln and p.Ter494Glu of *EFEMP1* gene was shown in **A** and **B**, respectively, with the Integrated Genome Viewer (IGV); the genotype of their parents was identified with Sanger sequencing. **C**, **D**: p.Arg387Gln and p.Ter494Glu for the father of the siblings, respectively. **E**, **F:** p.Arg387Gln and stop signal for the mother of the siblings, respectively. **G**: The pedigree map for the family with mutations in *EFEMP1*.

of sequence variants. The score of the prediction algorithm is usually based on the alteration of polarity, charge, and evolution conservation of amino acids. The predicted results might provide useful information for estimating the influence of these variants on protein function. However, the prediction of these variations on protein function might be inconsistent with the real context. In general, most algorithms for missense variant prediction are 65–80% accurate when examining known disease variants [25]. A further limitation of this study is that the sample size might not be large enough to detect all possible PDVs showing a statistically significant difference between patients and controls. Thus, these findings should be replicated in additional, larger cohorts. Therefore, additional cohort studies will be valuable for the identification of pathogenic alternations.

APPENDIX 1. PRIMARY OPEN ANGLE GLAUCOMA (POAG) SAMPLES INFORMATION AND THE POTENTIALLY DISEASE-RELEVANT VARIANTS (PDVS) IDENTIFIED IN POAG PATIENTS.

To access the data, click or select the words "Appendix 1."

APPENDIX 2. CONTROL SAMPLES INFORMATION AND PDVS IDENTIFIED IN CONTROL SUBJECTS.

To access the data, click or select the words "Appendix 2."

APPENDIX 3. THE LIST OF 26 CANDIDATE GENES FOR POAG IN THIS STUDY.

To access the data, click or select the words "Appendix 3."

APPENDIX 4. PRIMERS AND MOLECULAR INVERSION PROBES (MIPS) SEQUENCES.

To access the data, click or select the words "Appendix 4."

APPENDIX 5. OPTIMIZATION OF MIPS BASED ENRICHMENT AND SANGER SEQUENCING CONFIRMATION.

To access the data, click or select the words "Appendix 5."

APPENDIX 6. RARE VARIANTS IDENTIFIED IN POAG COHORT.

To access the data, click or select the words "Appendix 6."

APPENDIX 7. RARE VARIANTS IDENTIFIED IN CONTROL SUBJECTS.

To access the data, click or select the words "Appendix 7."

APPENDIX 8. RARE VARIANTS IDENTIFIED IN 1000-GENOME PROJECT (CHB AND CHS).

To access the data, click or select the words "Appendix 8."

APPENDIX 9. PDVS IN POAG AND CONTROL WITH MINOR ALLELE FREQUENCY (MAF) AND PREDICTION INFORMATION.

To access the data, click or select the words "Appendix 9."

APPENDIX 10. PDVS IDENTIFIED IN POAG AS COMPARED WITH CONTROL.

To access the data, click or select the words "Appendix 10."

APPENDIX 11. COST ESTIMATION FOR PANEL-SEQUENCING.

To access the data, click or select the words "Appendix 11."

ACKNOWLEDGMENTS

The work is supported by the project (No. 81670889) from the National Natural Science Foundation of China, the project (No. cstc2015jcyjBX0051) from the Natural Science Foundation of Chongqing, the project (Platform Enhancement of Radiation & Cancer Biology Laboratory) from Special funds for guiding local scientific and technological development by the central government of China, the project (Integrated innovation and application of key technologies for precise prevention and treatment of primary lung cancer) from Chongqing Municipal Health Committee, and the project (Technology platform construction of next generation sequencing and research on clinical translation) from Chongqing Cancer Institute. The funders only provided financial support and did not have any additional role in the study design, data collection and analysis, decision to publish, or manuscript preparation. **Ethics approval and consent to participate:** All patients gave their informed consent for their anonymized data to be submitted for audit and publication. The Ethics committee of the Third Affiliated Hospital (Daping Hospital) of the Army Medical University and the Research Institute of Surgery of the Academy of Military Medical Science (Medical research ethics approval No.49 (2017)). Dr. Tang (tang.cqcl@foxmail.com) and Dr. Shi (xshi.bear@foxmail.com) are co-corresponding authors for this paper.

REFERENCES

1. Abu-Amero K, Kondkar AA, Chalam KV. An updated review on the genetics of primary open angle glaucoma. Int J Mol Sci 2015; 16:28886-911. [PMID: 26690118].
2. Foris LA, Gossman WG. Glaucoma, open angle. StatPearls. Publishing Internet 2018.
3. Kumar S, Malik MA. K S, Sihota R, Kaur J. Genetic variants associated with primary open angle glaucoma in Indian population. Genomics 2017; 109:27-35. [PMID: 27851990].
4. Miller MA, Fingert JH, Bettis DI. Genetics and genetic testing for glaucoma. Curr Opin Ophthalmol 2017; 28:133-8. [PMID: 27898466].
5. Challa P. Glaucoma Genetics. Int Ophthalmol Clin 2008; 48:73-94. [PMID: 18936638].
6. Wang HW, Sun P, Chen Y, Jiang LP, Wu HP, Zhang W, Gao F. Research progress on human genes involved in the pathogenesis of glaucoma Mol Med Rep 2018; 18:656-74. Review[PMID: 29845210].
7. Liu Y, Allingham RR. Major review: Molecular Genetics of Primary Open-Angle Glaucoma. Exp Eye Res 2017; 160:62-84. [PMID: 28499933].
8. Stone EM, Fingert JH, Alward WL, Nguyen TD, Polansky JR, Sunden SL, Nishimura D, Clark AF, Nystuen A, Nichols BE, Mackey DA, Ritch R, Kalenak JW, Craven ER, Sheffield VC. Identification of a gene that causes primary open angle glaucoma. Science 1997; 275:668-70. [PMID: 9005853].
9. Alward WL, Fingert JH, Coote MA, Johnson AT, Lerner SF, Junqua D, Durcan FJ, McCartney PJ, Mackey DA, Sheffield VC, Stone EM. Clinical features associated with mutations in the chromosome 1 open-angle glaucoma gene (GLC1A). N EngI J Med 1998; 338:1022-7. [PMID: 9535666].
10. Rezaie T, Child A, Hitchings R, Brice G, Miller L, Coca-Prados M, Héon E, Krupin T, Ritch R, Kreutzer D, Crick RP, Sarfarazi M. Adult-onset primary open-angle glaucoma caused by mutations in optineurin. Science 2002; 295:1077-9. [PMID: 11834836].
11. Fan BJ, Wang DY, Cheng CY, Ko WC, Lam SC, Pang CP. Different WDR36 mutation pattern in Chinese patients with primary open-angle glaucoma. Mol Vis 2009; 15:646-53. [PMID: 19347049].
12. Badeeb OM, Micheal S, Koenekoop RK, den Hollander AI, Hedrawi MT. CYP1B1 mutations in patients with primary congenital glaucoma from Saudi Arabia. BMC Med Genet 2014; 15:109-13. [PMID: 25261878].
13. Sitorus R, Ardjo SM, Lorenz B, Preising M. CYP1B1 gene analysis in primary congenital glaucoma in Indonesian and European patients. J Med Genet 2003; 40:e9-[PMID: 12525557].
14. Fingert JH, Roos BR, Solivan-Timpe F, Miller KA, Oetting TA, Wang K, Kwon YH, Scheetz TE, Stone EM, Wallace LM. Analysis of ASB10 variants in open angle glaucoma. Hum Mol Genet 2012; 21:4543-8. [PMID: 22798626].
15. Pasutto F, Keller KE, Weisschuh N, Sticht H, Samples JR, Yang YF, Zenkel M, Schlötzer-Schrehardt U, Mardin CY, Frezzotti P, Edmunds B, Kramer PL, Gramer E, Reis A, Acott TS, Wirtz MK. Variants in ASB10 are associated with open-angle glaucoma. Hum Mol Genet 2012; 21:1336-49. [PMID: 22156576].
16. Strungaru MH, Dinu I, Walter MA. Genotype-phenotype correlations in Axenfeld-Rieger malformation and glaucoma patients with FOXC1 and PITX2 mutations. Invest Ophthalmol Vis Sci 2007; 48:228-37. [PMID: 17197537].
17. Mamanova L, Coffey AJ, Scott CE, Kozarewa I, Turner EH, Kumar A, Howard E, Shendure J, Turner DJ. Target-enrichment strategies for next-generation sequencing. Nat Methods 2010; 7:111-8. [PMID: 20111037].
18. O'Roak BJ, Vives L, Fu W, Egertson JD, Stanaway IB, Phelps IG, Carvill G, Kumar A, Lee C, Ankenman K, Munson J, Hiatt JB, Turner EH, Levy R, O'Day DR, Krumm N, Coe BP, Martin BK, Borenstein E, Nickerson DA, Mefford HC, Doherty D, Akey JM, Bernier R, Eichler EE, Shendure J. Multiplex Targeted Sequencing Identifies Recurrently Mutated Genes in Autism Spectrum Disorders. Science 2012; 338:1619-22. [PMID: 23160955].
19. Thorleifsson G, Magnusson KP, Sulem P, Walters GB, Gudbjartsson DF, Stefansson H, Jonsson T, Jonasdottir A, Jonasdottir A, Stefansdottir G, Masson G, Hardarson GA, Petursson H, Arnarsson A, Motallebipour M, Wallerman O, Wadelius C, Gulcher JR, Thorsteinsdottir U, Kong A, Jonasson F, Stefansson K. Common sequence variants in the LOXL1 gene confer susceptibility to exfoliation glaucoma. Science 2007; 317:1397-400. [PMID: 17690259].
20. Mackay DS, Bennett TM, Shiels A. Exome Sequencing Identifies a Missense Variant in EFEMP1 Co-Segregating in a Family with Autosomal Dominant Primary Open-Angle Glaucoma. PLoS One 2015; 10:e0132529-[PMID: 26162006].
21. Davis LK, Meyer KJ, Schindler EI, Beck JS, Rudd DS, Grundstad AJ, Scheetz TE, Braun TA, Fingert JH, Alward WL, Kwon YH, Folk JC, Russell SR, Wassink TH, Sheffield VC, Stone EM. Copy Number Variations and Primary Open-Angle Glaucoma. Invest Ophthalmol Vis Sci 2011; 52:7122-33. [PMID: 21310917].
22. Liu T, Xie L, Ye J, Liu Y, He X. Screening of candidate genes for primary open angle glaucoma. Mol Vis 2012; 18:2119-26. [PMID: 22876139].
23. Zhou T, Souzeau E, Siggs OM, Landers J, Mills R, Goldberg I, Healey PR, Graham S, Hewitt AW, Mackey DA, Galanopoulos A, Casson RJ, Ruddle JB, Ellis J, Leo P, Brown MA, MacGregor S, Sharma S, Burdon KP, Craig JE. Contribution of Mutations in Known Mendelian Glaucoma Genes to Advanced Early-Onset Primary Open-Angle Glaucoma. Invest Ophthalmol Vis Sci 2017; 58:1537-44. [PMID: 28282485].
24. Zhou T, Souzeau E, Sharma S, Siggs OM, Goldberg I, Healey PR, Graham S, Hewitt AW, Mackey DA, Casson RJ, Landers J, Mills R, Ellis J, Leo P, Brown MA, MacGregor S, Burdon KP, Craig JE. Rare variants in optic disc area gene CARD10

enriched in primary open-angle glaucoma. Mol Genet Genomic Med 2016; 4:624-33. [PMID: 27896285].

25. Richards S, Aziz N, Bale S, Bick D, Das S, Gastier-Foster J, Grody WW, Hegde M, Lyon E, Spector E, Voelkerding K, Rehm HL. ACMGLaboratory Quality Assurance Committee. Standards and guidelines for the interpretation of sequence variants: a joint consensus recommendation of the American College of Medical Genetics and Genomics and the Association for Molecular Pathology. Genet Med 2015; 17:405-24. [PMID: 25741868].

26. Kumar P, Henikoff S, Ng PC. Predicting the effects of coding non-synonymous variants on protein function using the SIFT algorithm. Nat Protoc 2009; 4:1073-81. [PMID: 19561590].

27. Adzhubei IA, Schmidt S, Peshkin L, Ramensky VE, Gerasimova A, Bork P, Kondrashov AS, Sunyaev SR. A method and server for predicting damaging missense mutations. Nat Methods 2010; 7:248-9. [PMID: 20354512].

28. Stoilova D, Child A, Brice G, Crick RP, Fleck BW, Sarfarazi M. Identification of a new 'TIGR' mutation in a family with juvenile-onset primary open angle glaucoma. Ophthalmic Genet 1997; 18:109-18. [PMID: 9361308].

29. Fingert JH, Heon E, Liebmann JM, Yamamoto T, Craig JE, Rait J, Kawase K, Hoh ST, Buys YM, Dickinson J, Hockey RR, Williams-Lyn D, Trope G, Kitazawa Y, Ritch R, Mackey DA, Alward WLM, Sheffield VC, Stone EM. Analysis of myocilin mutations in 1703 glaucoma patients from five different populations. Hum Mol Genet 1999; 8:899-905. [PMID: 10196380].

30. Aroca-Aguilar JD, Sanchez-Sanchez F, Ghosh S, Coca-Prados M, Escribano J. Myocilin mutations causing glaucoma inhibit the intracellular endoproteolytic cleavage of myocilin between amino acids arg226 and ile227. J Biol Chem 2005; 280:21043-51. [PMID: 15795224].

31. Kim H-J, Suh W, Park SC, Kim CY, Park KH, Kook MS, Kim YY, Kim C-S, Park CK, Ki C-S, Kee C. Mutation spectrum of CYP1B1 and MYOC genes in Korean patients with primary congenital glaucoma. Mol Vis 2011; 17:2093-101. [PMID: 21850185].

32. Alward WLM, Semina EV, Kalenak JW, Heon E, Sheth BP, Stone EM, Murray JC. Autosomal dominant iris hypoplasia is caused by a mutation in the Rieger syndrome (RIEG/PITX2) gene. Am J Ophthalmol 1998; 125:98-100. [PMID: 9437321].

33. Yoon SJK, Kim HS, Moon JI, Lim JM, Joo CK. Mutations of the TIGR/MYOC gene in primary open-angle glaucoma in Korea. Am J Hum Genet 1999; 64:1775-8. Letter[PMID: 10330365].

34. Donegan RK, Hill SE, Freeman DM, Nguyen E, Orwig SD, Turnage KC, Lieberman RL. Structural basis for misfolding in myocilin-associated glaucoma. Hum Mol Genet 2015; 24:2111-24. [PMID: 25524706].

35. Ito YA, Goping IS, Berry F, Walter MA. Dysfunction of the stress-responsive FOXC1 transcription factor contributes to the earlier-onset glaucoma observed in Axenfeld-Rieger syndrome patients. Cell Death Dis 2014; 5:e1069-[PMID: 24556684].

36. Doucette LP, Rasnitsyn A, Seifi M, Michael A, Walter MA. The interactions of genes, age, and environment in glaucoma pathogenesis. Surv Ophthalmol 2015; 60:310-26. [PMID: 25907525].

37. Chen Y, Cai J, Jones DP. Mitochondrial thioredoxin in regulation of oxidant-induced cell death. FEBS Lett 2006; 580:6596-602. [PMID: 17113580].

38. Lattante S, Millecamps S, Stevanin G, Rivaud-Péchoux S, Moigneu C, Camuzat A, Da Barroca S, Mundwiller E, Couarch P, Salachas F, Hannequin D, Meininger V, Pasquier F, Seilhean D, Couratier P, Danel-Brunaud V, Bonnet AM, Tranchant C, LeGuern E, Brice A, Le Ber I, Kabashi E. French Research Network on FTD and FTD-ALS. Contribution of ATXN2 intermediary polyQ expansions in a spectrum of neurodegenerative disorders. Neurology 2014; 83:990-5. [PMID: 25098532].

39. Mears AJ, Jordan T, Mirzayans F, Dubois S, Kume T, Parlee M, Ritch R, Koop B, Kuo WL, Collins C, Marshall J, Gould DB, Pearce W, Carlsson P, Enerbäck S, Morissette J, Bhattacharya S, Hogan B, Raymond V, Walter MA. Mutations of the forkhead/winged-helix gene, FKHL7, in patients with Axenfeld–Rieger anomaly. Am J Hum Genet 1998; 63:1316-28. [PMID: 9792859].

40. Bailey JN, Loomis SJ, Kang JH, Allingham RR, Gharahkhani P, Khor CC, Burdon KP, Aschard H, Chasman DI, Igo RP Jr, Hysi PG, Glastonbury CA, Ashley-Koch A, Brilliant M, Brown AA, Budenz DL, Buil A, Cheng CY, Choi H, Christen WG, Curhan G, De Vivo I, Fingert JH, Foster PJ, Fuchs C, Gaasterland D, Gaasterland T, Hewitt AW, Hu F, Hunter DJ, Khawaja AP, Lee RK, Li Z, Lichter PR, Mackey DA, McGuffin P, Mitchell P, Moroi SE, Perera SA, Pepper KW, Qi Q, Realini T, Richards JE, Ridker PM, Rimm E, Ritch R, Ritchie M, Schuman JS, Scott WK, Singh K, Sit AJ, Song YE, Tamimi RM, Topouzis F, Viswanathan AC, Verma SS, Vollrath D, Wang JJ, Weisschuh N, Wissinger B, Wollstein G, Wong TY, Yaspan BL, Zack DJ, Zhang K, Study EN. ANZRAG Consortium. Weinreb RN, Pericak-Vance MA, Small K, Hammond CJ, Aung T, Liu Y, Vithana EN, MacGregor S, Craig JE, Kraft P, Howell G, Hauser MA, Pasquale LR, Haines JL, Wiggs JL. Genome-wide association analysis identifies TXNRD2, ATXN2 and FOXC1 as susceptibility loci for primary open-angle glaucoma. Nat Genet 2016; 48:189-94. [PMID: 26752265].

41. Suriyapperuma SP, Child A, Desai T, Brice G, Kerr A, Crick RP, Sarfarazi M. A new locus (GLC1H) for adult-onset primary open-angle glaucoma maps to the 2p15-p16 region. Arch Ophthalmol 2007; 125:86-92. [PMID: 17210857].

42. Stone EM, Lotery AJ, Munier FL, Héon E, Piguet B, Guymer RH, Vandenburgh K, Cousin P, Nishimura D, Swiderski RE, Silvestri G, Mackey DA, Hageman GS, Bird AC, Sheffield VC, Schorderet DF. A single EFEMP1 mutation associated with both Malattia Leventinese and Doyne honeycomb retinal dystrophy. Nat Genet 1999; 22:199-202. [PMID: 10369267].

43. Narendran N, Guymer RH, Cain M, Baird PN. Analysis of the EFEMP1 gene in individuals and families with early onset drusen. Eye (Lond) 2005; 19:11-5. [PMID: 15218514].

44. Meyer KJ, Davis LK, Schindler EI, Beck JS, Rudd DS, Grundstad AJ, Scheetz TE, Braun TA, Fingert JH, Alward WL, Kwon YH, Folk JC, Russell SR, Wassink TH, Stone EM, Sheffield VC. Genome-wide analysis of copy number variants in age-related macular degeneration. Hum Genet 2011; 129:91-100. [PMID: 20981449].

45. Lin Y, Liu T, Li J, Yang J, Du Q, Wang J, Yang Y, Liu X, Fan Y, Lu F, Chen Y, Pu Y, Zhang K, He X, Yang Z. A genome-wide scan maps a novel autosomal dominant juvenile-onset open-angle glaucoma locus to 2p15–16. Mol Vis 2008; 14:739-44. [PMID: 18432317].

Articles are provided courtesy of Emory University and the Zhongshan Ophthalmic Center, Sun Yat-sen University, P.R. China. The print version of this article was created on 21 May 2020. This reflects all typographical corrections and errata to the article through that date. Details of any changes may be found in the online version of the article.